Article

Hydrogen Storage Capacity of Tetrahydrofuran and Tetra-*N*-Butylammonium Bromide Hydrates Under Favorable Thermodynamic Conditions

Joshua T. Weissman [1] and Stephen M. Masutani [2,*]

[1]   Hawaiian Electric Company, Honolulu, HI 96814, USA; josh.weissman@hawaiianelectric.com
[2]   Hawaii Natural Energy Institute, University of Hawaii, Honolulu, HI 96822, USA
*   Correspondence: stephenm@hawaii.edu; Tel.: +1-808-956-7388

Abstract: An experimental study was conducted to evaluate the feasibility of employing binary hydrates as a medium for H_2 storage. Two reagents, tetrahydrofuran (THF) and tetra-*n*-butylammonium bromide (TBAB), which had been reported previously to have potential to form binary hydrates with H_2 under favorable conditions (i.e., low pressures and high temperatures), were investigated using differential scanning calorimetry and Raman spectroscopy. A scale-up facility was employed to quantify the hydrogen storage capacity of THF binary hydrate. Gas chromatography (GC) and pressure drop analyses indicated that the weight percentages of H_2 in hydrate were less than 0.1%. The major conclusions of this investigation were: (1) H_2 can be stored in binary hydrates at relatively modest pressures and temperatures which are probably feasible for transportation applications; and (2) the storage capacity of H_2 in binary hydrate formed from aqueous solutions of THF over a concentration range extending from 2.78 to 8.34 mol % and at temperatures above 263 K and pressures below 11 MPa was <0.1 wt %.

1. Introduction

While the majority of hydrate research funding and activities currently are directed toward investigations of natural gas hydrates, there is interest in hydrate storage of H_2 for transportation applications [1,2]. Pure H_2 hydrate requires very high pressures, which makes them impractical under most storage scenarios [1–3]. In order to reduce the prohibitively high pressure requirement, H_2 mixed gas hydrates have been investigated [1–5]. Hashimoto et al. [6] demonstrated that adding small amounts of tetra-*n*-butylammonium bromide (TBAB; $C_{16}H_{36}NBr$) to water reduced the hydrogen hydrate formation pressure from 350 MPa to ~1 MPa at 280 K. TBAB is a salt that forms a semi-clathrate hydrate crystal ($C_{16}H_{36}N^+ \cdot Br^- \cdot 38H_2O$) at atmospheric pressure and near room temperature with a unit-cell composed of 16 small (S)-cages and eight large (L)-cages. The bromide anion forms cage structures with water molecules while the cation occupies empty L-cages [7]. At moderate pressures and temperatures (e.g., 1 MPa and 280 K), hydrogen molecules can be stabilized and trapped within available empty S-cages [8].

Tetrahydrofuran (THF; C_4H_8O) has also been reported to reduce hydrogen hydrate formation pressures [8–10]. THF is a water miscible organic liquid compound that generates structure II (sII) hydrates at 278 K at 0.1 MPa [11]. The ideal composition of a THF hydrate is 17 mol H_2O per mol THF [12] or about 5.56 mol % THF. According to Lee et al. [8], THF hydrate can store about 4 wt % H_2 at 12 MPa and 270 K; however, experiments by Ogata et al. [13] suggest that, under similar conditions, stoichiometric THF hydrate can store only 0.26 wt % H_2.

Hydrogen is the most abundant element in the universe and can be produced from natural gas and other hydrocarbons, or by electrolysis of water. H_2 is the fuel of choice for many types of fuel cells under development for propulsion and power generation applications [14,15]. Employing hydrogen hydrate as an energy carrier has attracted interest [3–5], primarily since oxidation of H_2 produces no greenhouse gas carbon emissions (although H_2 produced by reforming or pyrolysis of hydrocarbon fuels does have an associated carbon footprint).

One of the primary advantages of H_2 hydrate storage for propulsion applications is that, unlike metal hydrides, which must undergo a chemical reaction (often having slow kinetics and requiring heating up to 473 K) to release hydrogen fuel [16], hydrates undergo a rapid, on-demand, phase transformation (i.e., melting), making them ideal for onboard use in fuel cell vehicles and other specialized applications.

The greatest uncertainty related to onboard hydrogen hydrate storage for propulsion is energy density. The U.S. Department of Energy previously set a 2015 target of 5.5 wt % hydrogen storage in hydrates [17,18]. Theoretical studies performed to date by Willow and Xantheas [19] suggest that hydrates may be able to store up to 5.3 wt % hydrogen; however, limited experimental data exist to validate these results.

Since binary hydrates, such as those employing THF and TBAB, can store H_2 at considerably lower pressure than pure H_2 hydrate, the overall goal of this study was to explore whether these hydrates represent a viable medium for H_2 storage. Candidate protocols to form binary hydrogen hydrates at relatively low formation pressure and high formations temperatures were identified via a series of exploratory experiments that employed a Differential Scanning Calorimeter (DSC) and Raman spectroscopy system. Since earlier studies of the hydrogen storage capacity of binary H_2 hydrates have produced conflicting results, it was important to quantify this parameter. H_2 wt % could not be accurately determined in the small-scale DSC tests, so these formation protocols were scaled up to produce samples large enough to measure the hydrogen content (gm H_2/gm hydrate) of the selected binary hydrates.

2. Materials and Methods

2.1. Materials

A Multi-Cell Differential Scanning Calorimeter (MCDSC, TA Instruments, Lindon, UT, USA) was used to identify candidate protocols to form binary hydrogen hydrates at moderate temperatures and pressures. Binary H_2 hydrates were formed in the calorimeter sample cell using various solutions of THF and TBAB at different pressures. The MCDSC is equipped with three sample cells and one reference cell, allowing the user to perform multiple tests simultaneously. It can detect heat flows down to about 0.2 µW. A schematic diagram of the MCDSC system employed in this investigation is provided in Figure 1.

The MCDSC is equipped with four thermo-electric-device (TED) detectors which are mounted to a shared heat sink and controlled by a resistance temperature detector (RTD) sensor or scanned by the Scan TED. A 1 kΩ platinum RTD (F) monitors the DSC temperature. Precise temperature control over the range of 233 K–423 K is achieved using a combination of an electric heater and a cascade of Peltier coolers along with a circulating water bath which serves as a hot side reference for the cooler. The 17.2 mm o.d. × 16.6 mm tall cylindrical sample cells (ampoules) have an internal volume of 0.5 mL and are made of Hastelloy. Maximum operating pressure is 41.5 MPa (6000 psig). Figure 2 is a photograph of a sample cell showing the top closure that is fitted with a tube that allows the addition or removal of different gases (e.g., H_2) during experiments.

Research Grade 4.8 (99.998% purity) N_2 and ultra-high purity grade 5.0 (99.999% purity) H_2 were employed in these experiments. N_2 was used to purge the system of oxidizing gas before addition of the combustible H_2. Dry N_2 gas also is constantly circulated within the calorimeter to prevent

condensation from occurring when operating at temperatures below the dew point of the ambient air. H_2 was used to form the gas hydrates.
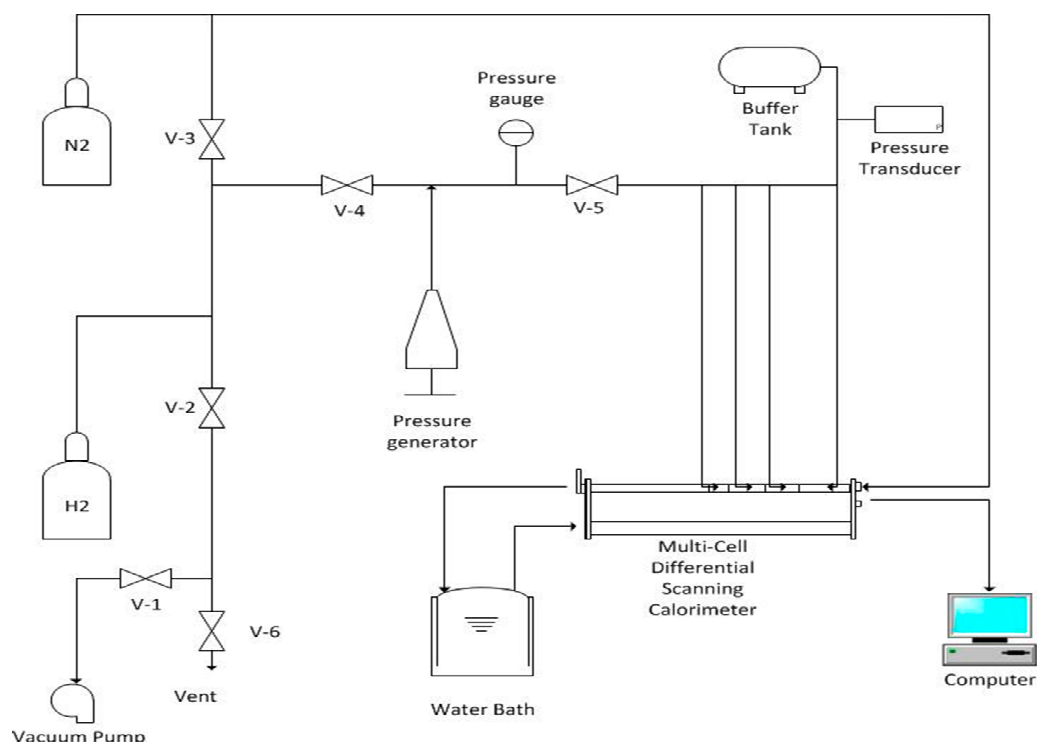

Figure 1. Schematic drawing of the calorimeter setup.

Figure 2. Photograph of the MCDSC high pressure sample cell and closure.

Since the commercial gas cylinder pressure was 13.8 MPa, a manual pressure generator from High Pressure Equipment Company (Erie, PA, USA was utilized to increase the pressure of the sample above this value. The pressure generator has a stroke capacity of 60 cm^3 per stroke and a maximum working pressure of 34 MPa. A 100 cm^3 buffer tank (i.e., high pressure stainless steel gas reservoir) was used to minimize pressure swings in the sample cell during the experiment due to the consumption of gas during hydrate formation or to compensate for small leakages from valves and connections. System pressure was monitored with both a Bourdon tube pressure gauge and an electronic pressure transducer (model PX309, Omega Engineering, Stamford, CT, USA. The pressure transducer had an operating range of 0 to 13.8 MPa and an accuracy of 2% full-scale.

While the calorimeter thermograms could confirm solidification and melting events in the DSC sample cells, Raman spectroscopy was employed to verify that the solid phase included binary hydrogen hydrate. A schematic diagram of the Raman system used in our experiments is provided in Figure 3. Components of the system have been used in previous hydrate studies conducted with a BT2.15 DSC (Setaram, Hillsborough, NJ, USA) modified to perform simultaneous calorimetry and Raman spectroscopy. In the present experiments, binary hydrate was formed in a 12 mL internal volume, cylindrical high pressure mixing cell from the Setaram BT2.15 DSC that was immersed in a precision temperature water bath. The top closure of the mixing cell has been modified to allow insertion of a fiber optic probe that comprises seven 200 μm core UV silica fibers encased in epoxy within a 3.18 mm (0.125 in.) o.d. stainless steel tube. Figure 4 shows photograph and a cross sectional diagram of the fiber optic probe assembly. The probe passes through a 6.4 mm (0.25 in.) stainless steel tube attached at one end with a compression fitting to the top closure of the mixing cell and at the other to a machined stainless steel block that also serves as a manifold for gases that can be added or extracted from the sample cell.
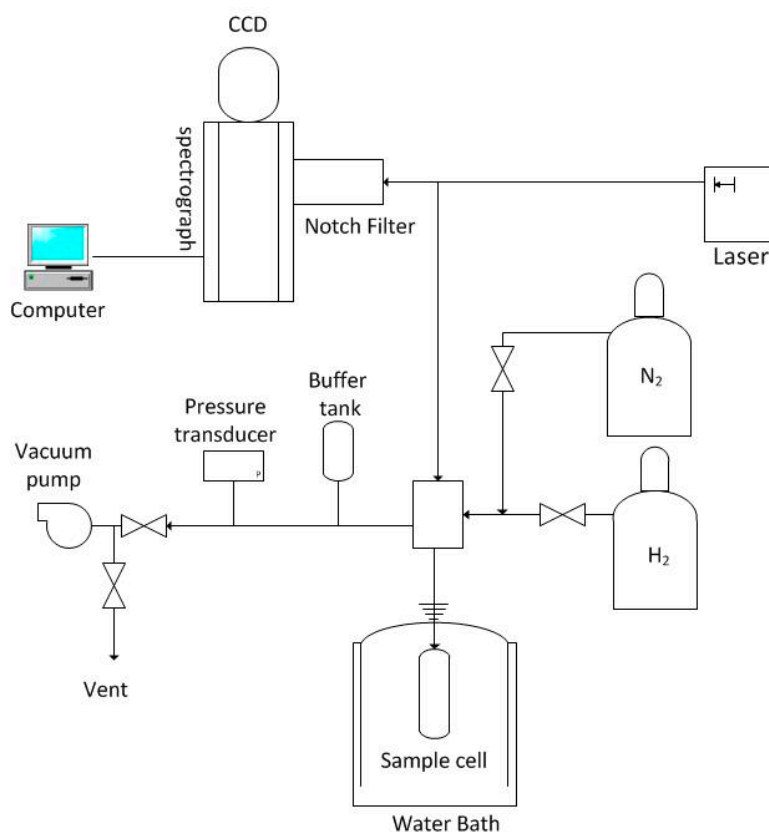

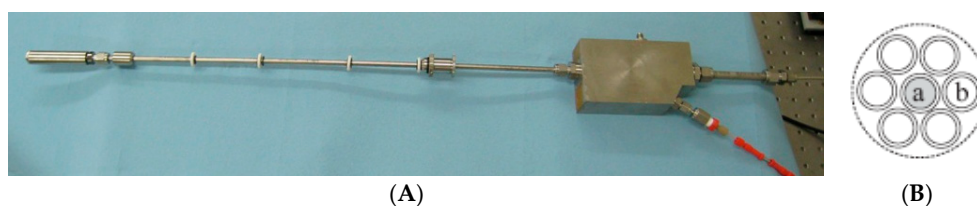**Figure 3.** Diagram of the Raman spectroscopy facility.

Figure 4. Photograph (**A**) and cross-sectional view (**B**) of the fiber optic probe. Light from the laser is transmitted into the sample cell by fiber (a) the surrounding six fibers; (b) collect scattered light.

The output from a 532 nm diode-pumped, 100 mW solid-state laser is coupled to the center fiber of the fiber optic probe (fiber (a) in Figure 4) and transmitted into the sample cell. Raman shifted radiation from the material in the cell is collected by the six other fibers of the probe (fibers (b) in Figure 4) and transmitted to the spectrometer. A notch filter removes reflected laser radiation at 532 ± 0.6 nm prior to entering the SpectraPro-2750 (Princeton Instruments, Trenton, NJ, USA) with a focal length of 0.750 m. A Princeton Instruments PIXIS 2 K (Model number 7533-0001) camera detector equipped with a 2048×512 pixel imaging array is used to record the Raman signal.

The calorimeter and Raman facilities examine small samples of hydrate, typically of the order of a few cm^3 or less. Quantitative measurements of H_2 content by analysis of gas collected after decomposing the hydrate are difficult to perform accurately with such small quantities. Consequently, a scale-up hydrate synthesis facility, shown schematically in Figure 5, was constructed for this purpose. The facility has a maximum working pressure of 17 MPa. The operating temperature range is 243 K to 298 K.
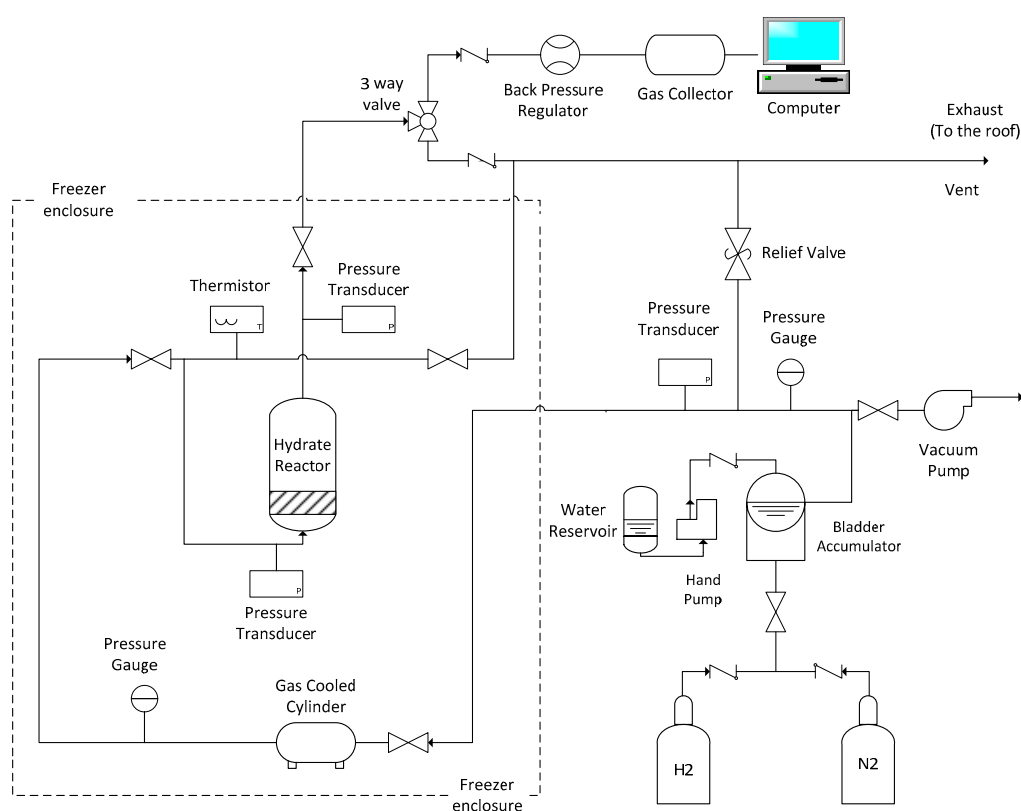

Figure 5. Layout of the scale up facility.

Hydrate samples are formed in a tubular series reactor (High Pressure Equipment Company, Model TOC-20) inside a laboratory freezer shown in Figure 6. The stainless steel tubular reactor has an internal volume of 0.5 L and maximum working pressure of 34 MPa. A 51 cm long PTFE tube with and i.d. of 4 cm is inserted into the reactor to isolate the hydrate samples from the reactor walls. Pressure is monitored with Omega Engineering pressure transducers (PT) (model PX309) teed into lines connected to both the upper and lower closures of the reactor. Gas temperature is monitored with a thermistor (Omega Engineering Model TJ36-44004) inserted into the gas line emerging from the lower closure. Pressurized gases used to purge the system or to form the hydrate are precooled inside two 300 cm^3 buffer tanks (i.e., stainless steel sample cylinders) located behind the reactor in freezer. Precooling minimizes changes in temperature of the sample during the experiment. Gas flow into the reactor is controlled using the panel shown on the right hand side of the photograph in Figure 6.
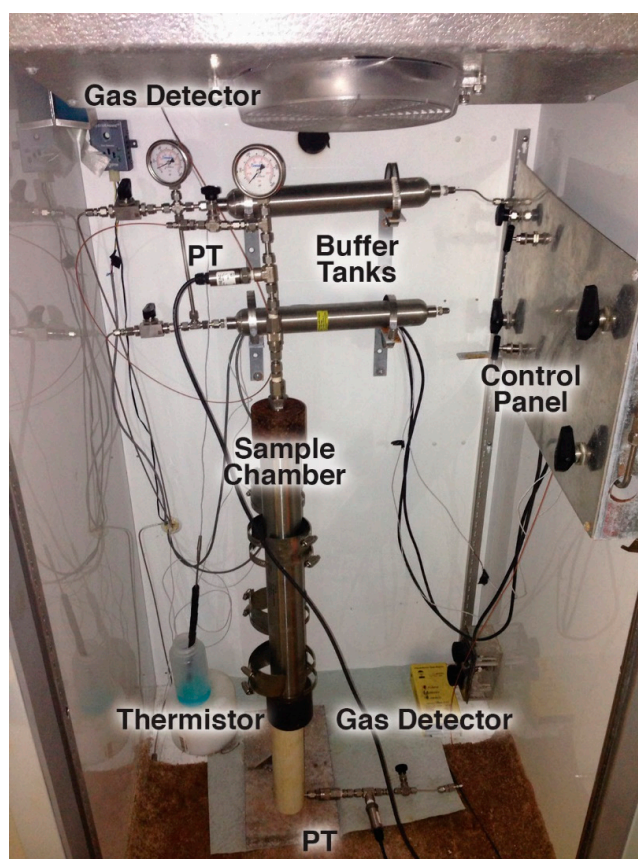
Figure 6. Photograph of the hydrate scale-up sample chamber.

It was necessary to increase the pressure of the purge N_2 gas and H_2 gas used to form the hydrate above levels in the commercial gas cylinders. A bladder accumulator was employed for this purpose. Outside the freezer, bottled N_2 or H_2 gas flows into the shell of a 1 gallon accumulator. Water is pumped manually from a reservoir into an elastomer bladder contained inside the metal accumulator shell. As the bladder expands, it compresses the surrounding gas in the shell, increasing its pressure. Pressurized gas exits from the bottom of the accumulator and fills the buffer tanks inside the freezer.

After hydrate is formed in the sample chamber and before it is decomposed to collect the released gas, the head space in the chamber and the gas lines are purged with N_2 to eliminate as much of the H_2 gas as possible, since residual H_2 complicates the determination of the hydrogen content of the hydrate. Care is exercised to minimize variations in the sample pressure (by means of a back pressure regulator) and temperature (by using precooled gas from the buffer tank) during the purge. After the lines and headspace are cleared of H_2, the system is brought to room temperature to allow the hydrate to fully dissociate. Flow exits the top of the sample chamber and passes through a 3-way valve that directs the gas either to collection chambers or a vent line. There are two collection ports: one to take 50 cm^3 samples and another to collect 3.8L samples. Gas samples collected during the purge and after hydrate decomposition are analyzed with a Shimadzu (Kyoto, Japan) model 14A gas chromatograph (GC). Helium was employed as a carrier to transport the sample gas through the GC separation column. A thermal conductivity detector (TCD) identified gas species in the eluted sample.

2.2. Methods

Aqueous solutions used to form binary H_2 gas hydrates were prepared by mixing distilled and deionized water with quantities of reagent grade THF (99.99%) or TBAB (99.99%). In this study,

three different concentrations of THF (2.78, 5.56 and 8.34 mol %) and two concentrations of TBAB (1.38 and 3.59 mol %) were investigated at gauge pressures of 0, 6.89, 10.34 and 13.79 MPa.

The apparatus shown in Figure 7 was used to generate hydrate particles from the THF or TBAB solutions. The white PVC column is filled with a solution of THF or TBAB and closed. An aerosol spray is generated from a nozzle installed in the bottom of the column by pressurization of the liquid with N_2 gas. Directly beneath the nozzle is a bucket containing liquid N_2. Tiny droplets of the solution contact the cold liquid N_2 and immediately form hydrate particles. The particles are collected and placed inside a laboratory freezer held at 262 K that is equipped with a glove. A set of sieves were used to size sort the hydrate crystals. Particles ≤ 210 μm were used in the experiments.

Figure 7. Apparatus used to generate THF and TBAB hydrate crystals.

To form H_2 binary hydrates, a pressure cell is loaded with either liquid THF or TBAB solution or the fine hydrate crystals produced from these solutions and slowly pressurized with ultra-high purity Grade 5.0 H_2 gas. Prior to pressurizing the cells, the system is purged with Grade 4.8 N_2 and evacuated with a vacuum pump to remove any oxidizing gases. Combustible gas detectors are installed in the laboratory to monitor for leaks.

2.2.1. MCDSC Experiments

The MCDSC requires sample cells to be loaded into the instrument at room temperature. This prevents condensation from occurring in the calorimeter and affecting the thermo-electric detectors, but also precludes the use of fine THF or TBAB crystals which will quickly melt. Hence, for the MCDSC experiments, binary gas hydrates were formed from liquid solutions of THF or TBAB.

The MCDSC sample cells were filled with a recorded mass of solution (approximately 0.25 g) and placed into the thermal well of the calorimeter. Gas lines were purged with N_2, then evacuated with a vacuum pump, and finally pressurized with H_2. Each of the five THF and TBAB solutions were tested at gauge pressures of 0, 6.89, 10.34 and 13.79 MPa.

The temperature time-history shown in Figure 8 was applied to cycle the samples between 263 K and 293 K (-10 °C and 20 °C). Binary hydrate nucleation and growth occurs as the solution is cooled from room temperature to 263 K at a rate of 2 K/min and held for two hours. Ice formation also occurs. Next, the samples are allowed to fully dissociate by increasing the temperature from 263 K to 293 K at a rate of 0.1 K/min. This thermal cycling is repeated two more times to minimize any start-up transients and maximize hydrate yield.
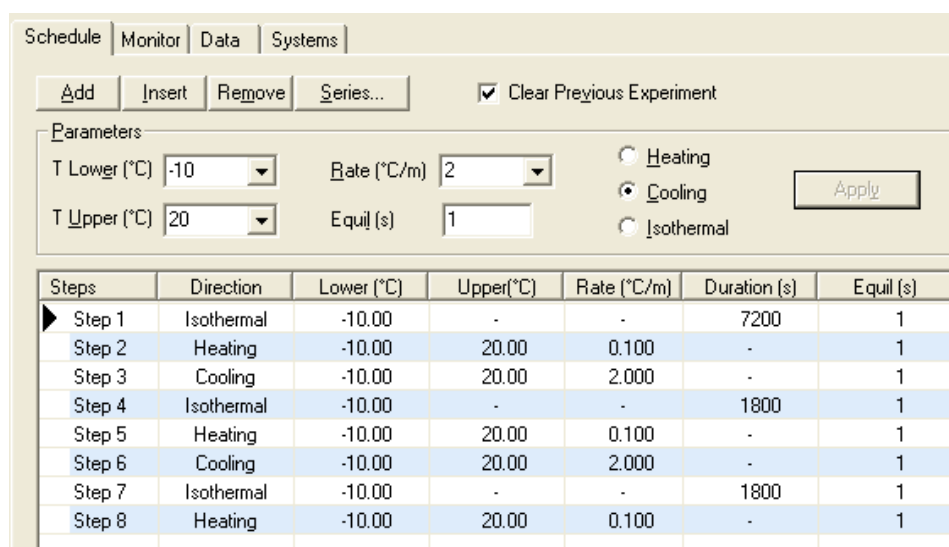
Figure 8. Temperature history for MCDSC experiments.

2.2.2. Confirmation of Binary H_2 Hydrate by Raman Spectroscopy

Candidate TBAB and THF solutions to form H_2 binary hydrates identified from the MCDSC thermograms were verified using Raman spectroscopy. Spectra of the tested samples were taken for the three different phases that exist in the cell: liquid, gas and hydrate.

In these experiments, fine THF or TBAB hydrate crystals were synthesized following the procedures described above. Approximately 10 g of crystals were loaded into the larger 12 mL pressure cell. The top closure of the cell was secured and the cell was submerged in a water bath circulating a solution of ethylene glycol at 263 K. The sample was then slowly pressurized with H_2 to 10.34 MPa. A magnetic stirrer inside the cell was employed to agitate the liquid sample before being turned off.

Initially, the sample was held at 263 K for 24 h, allowing gas to diffuse into the hydrate cages. Next, the sample temperature was increased to 285 K and held for 4 h. During this period, the gas hydrates start to dissociate and form a liquid-gas interface. A Raman spectrum of the sample was taken at this stage of the process.

Gas hydrates were reformed by lowering the sample temperature to 274 K and holding for 4 h. A Raman measurement was performed to verify hydrate formation. Finally, the sample was vented and brought to ambient conditions and one last spectrum was collected of the aqueous solution in the cell. Each of the spectra has a central wavelength of 685 nm using an 1800 nm grating.

2.2.3. Scale-Up Experiments

THF hydrate crystals were sieved down to a size of 210 μm and the crystals were loaded into the 4 cm i.d. PTFE tube to provide a permeable matrix for the H_2 gas. The mass of the hydrate crystals next was measured with a precision balance. The tube was loaded into the stainless steel tubular reactor located inside the freezer. Freezer temperature was set at 263 K. Gas flows through the hydrate crystals via a concentric stainless steel 6.4 mm (1/4″) O.D. tube. The sample was slowly pressurized with precooled H_2 and held at 263 K for 12 h. Next, the sample was slowly warmed to 277 K and held for 4 h, allowing any ice that formed to melt. Finally, conversion of the remaining liquid to hydrate was allowed to proceed for 24 h at 274 K.

After 24 h, the hydrate was dissociated and the released gas was collected to determine how much H_2 was stored in the binary hydrate. In order to do this, the H_2 gas surrounding the hydrate in the sample chamber and in the connected gas system must first be removed, since this inventory would overwhelm the H_2 released from the hydrate. A protocol was developed for this purpose and Figure 9

shows the various stages of the gas collection process. At State 1, the sample chamber and lines contain pressurized H_2 gas. Between State 1 and State 2, chilled Grade 4.8 N_2 gas is used to purge all or most of the H_2 gas that didn't get trapped in the hydrate phase from the system. During this purge process, a 1 gallon (3.785 L) gas sampling cylinder is used to collects of mixed hydrogen and nitrogen gas at a pressure of approximately 7 MPa for later analysis. Smaller samples are also collected at various points in the purge process to confirm that most of the H_2 has been removed. To ensure that there are no significant deviations in system pressure which might lead to hydrate decomposition, the back pressure regulator shown in the Figure is set to the initial sample pressure. At State 3, following the purge, the freezer is turned off and the door is opened to allow the hydrate to fully dissociate at room temperature for 24 h. As the hydrate dissociates, the trapped H_2 gas is released from hydrate cages, and mixes with the N_2 in the chamber and lines. This gas mixture is collected in sampling cylinders and analyzed using a Shimadzu 14-A GC.
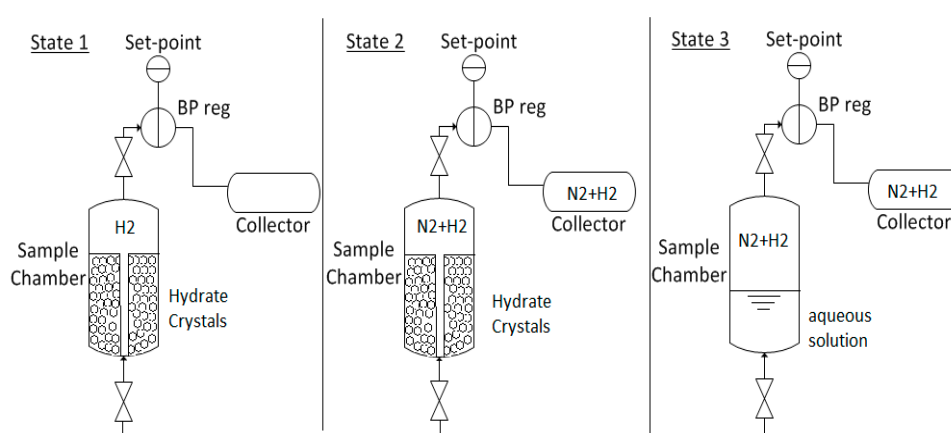

Figure 9. Gas purge and sample collection process.

The measured H_2 concentrations in the various gas samples are used to determine the quantity of H_2 stored in hydrate. This is compared with data on the pressure drop that occurs during hydrate formation due to H_2 uptake.

3. Results

3.1. Calorimetry

The objective of the MCDSC experiments was to identify the best candidates to form binary hydrogen hydrates. Three different aqueous solutions of THF (2.78, 5.56 and 8.34 mol %) and two of TBAB (1.38 and 3.59 mol %) were compared at H_2 pressures of 6.89, 10.37 13.79 MPa (gauge). In these tests, during the last stage of the programmed cooling and heating process shown in Figure 8, the calorimeter sample temperature was slowly ramped from 263 K to 293 K at a constant rate of 0.1 K/min. Triplicate experiments were performed for each concentration of THF and TBAB.

Calorimeter thermograms of the final hydrate (and ice) decomposition (heating) step, for 2.78, 5.56 and 8.34 mol % THF, are shown in Figures 10–12, respectively. While the calorimeter measures the rate of heat flow (µJ/s) to or from a sample, we have divided these data by the measured mass of the initial liquid solution in each cell, to account for small variations of this quantity between samples, and also the user-selected temperature ramping rate (0.1 K/min). This results in a parameter with the same units as specific heat capacity (J/kg-K) but which, in this case, includes both the sensible and latent heat components of the material comprising the sample. This parameter is plotted as a function of temperature, where endothermic processes correspond to positive values.
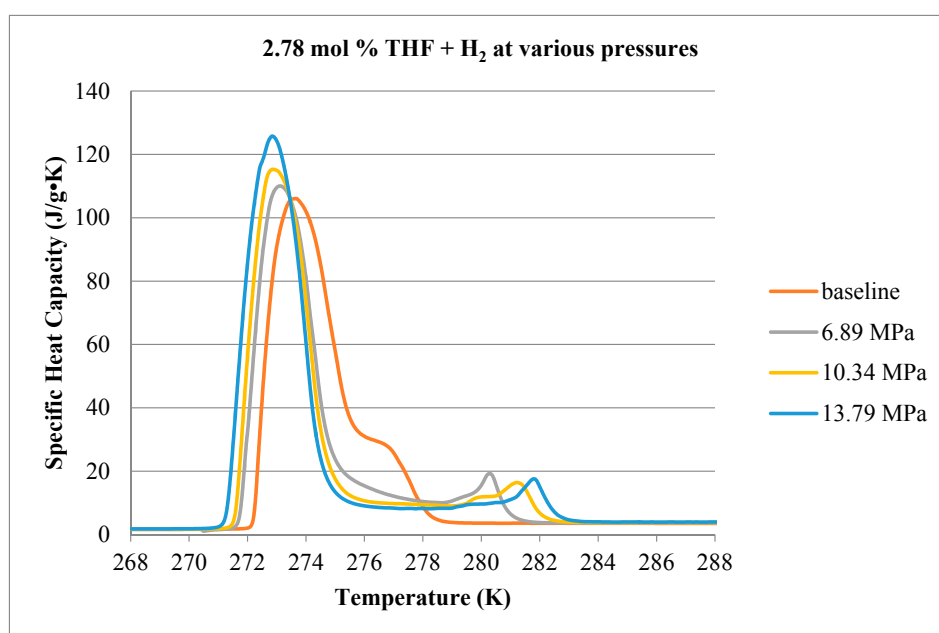
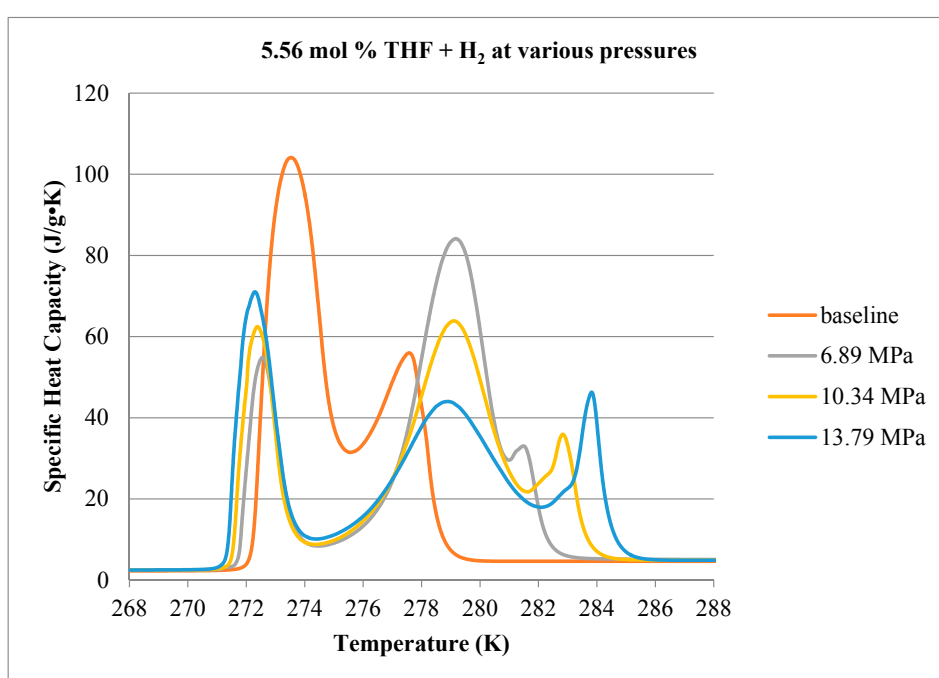**Figure 10.** Comparison of decomposition curves for 2.78 mol % THF at various hydrogen pressures.

Figure 11. Comparison of decomposition curves for 5.56 mol % THF at various hydrogen pressures.
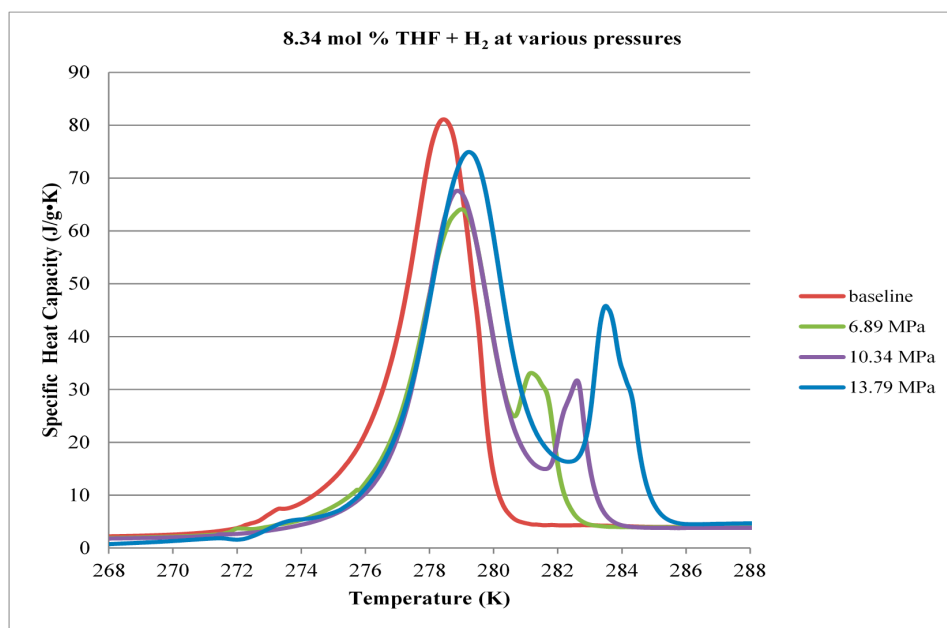
Figure 12. Comparison of decomposition curves for 8.34 mol % THF at various hydrogen pressures.

An initial test was conducted at atmospheric pressure (without H_2 addition) as a baseline. At 2.78 mol % THF, the solution contains about half the THF required to form pure hydrate [12]. Figure 10 shows a large endothermic peak with a small shoulder to the right. For the atmospheric pressure case, the apex of the large peak occurs at approximately 273.5 K and corresponds to ice melting. The small shoulder to the right of the ice peak is associated with the THF hydrate and its apex occurs at 277 K. As H_2 pressure in the cell increases, the binary hydrate peak decouples from the ice peak and moves to higher temperatures. As expected, the ice melting peak shifts to lower temperatures with increasing pressure.

Results for 5.56 mol % THF are shown in Figure 11. All thermograms exhibit a large endothermic peak near 273 K, indicating that ice continues to form even though the solution contains sufficient THF to ensure no excess water. The second peak between 277 K and 280 K occurs for the no-H_2 case (i.e., 0 MPa gauge pressure) and is believed to represent decomposition of pure THF hydrate. As the sample is pressurized with H_2, a small shoulder appears at higher temperatures to the right of the THF peak, possibly due to the dissociation of hydrogen hydrate. To test this, a calorimetry experiment was performed where a 5.56 mol % THF solution was pressurized to 10.34 MPa with pure N_2 gas. The measured thermogram is compared with the thermogram of the 5.56 mol % THF solution pressurized with H_2 in Figure 13. In the absence of H_2, the third peak to the right of the THF peak does not appear. There is, however, another new peak, this time to the left of the THF hydrate peak which may reflect the presence of N_2 in the solid phase.

When THF concentration in the solution was increased to 8.34 mol %, the ice melting peak in the thermograms disappears, as seen in Figure 12. All of the solution is converted to hydrate. The two remaining endothermic events (indicated by the two peaks) correlate well with thermograms obtained at 5.56 mol % THF.

The fraction of the solution that forms hydrate at different pressures can be estimated by deconvolving the ice and hydrate peaks, and calculating the area under the ice peak and above a baseline that accounts for the sensible heat component of the sample. Different algorithms to determine the sensible heat baseline from the thermograms were tested and are discussed by Weissman [20]. The area under the ice peak can be multiplied by the sample mass to obtain the total energy required to melt the ice component. Dividing this by literature values of the latent heat of pure water ice, ΔH_f, yields the mass of the ice component,

which is then subtracted from the total mass of the sample. Following this approach, about 35% of the 5.56 mol % THF solution is converted into hydrate at atmospheric pressure. Pressurizing the sample with H_2 gas increases this percentage to 75%, 76%, and 78% at 6.89, 10.34, and 13.79 MPa, respectively.
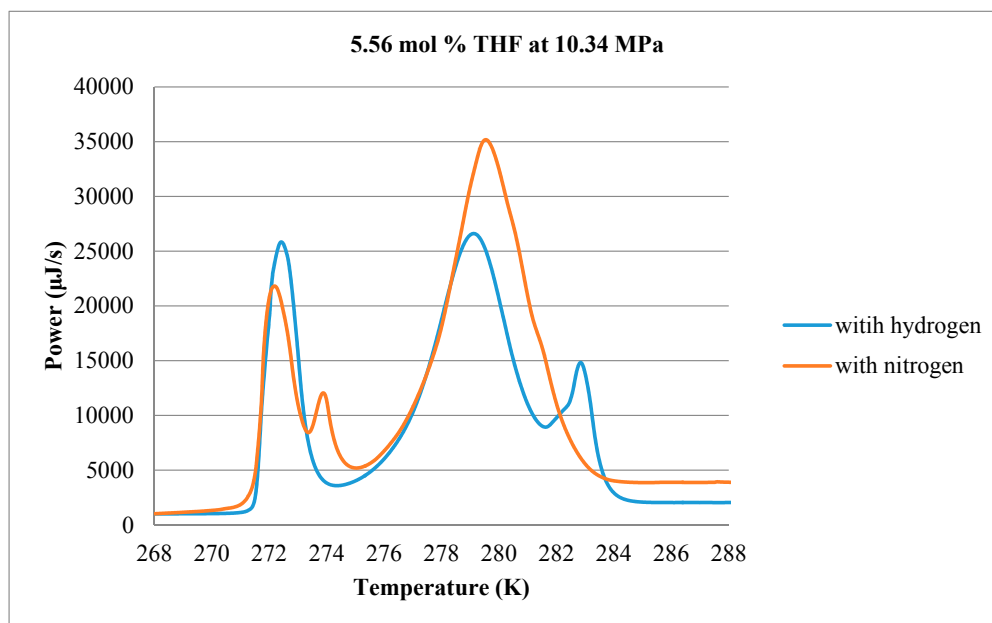

Figure 13. Comparison of ice and hydrate decomposition thermograms for 5.56 mol % THF at 10.34 MPa under pure N_2 (red) and pure H_2 (blue) gas.

Calorimetry results for binary hydrate formed from aqueous solutions of TBAB are shown in Figures 14 and 15. TBAB has been proposed to reduce the formation pressure of H_2 hydrate [6,21,22]. TBAB is known to form semi-clathrate hydrate in which the water cage is broken to accommodate the large TBAB molecule [23]. The ratio of TBAB:water in the hydrate has been reported to range from 1:2 to 1:36. 20% and 40% by mass solutions of TBAB were investigated which correspond to 1.38 mol % (~1:72) and 3.59 mol % (~1:27), respectively.

The thermograms in Figure 14, obtained using 1.38 mol % TBAB solution, exhibit two endothermic peaks, similar to the 2.78 mol % THF case. It can be surmised that the strong peak to the left corresponds to the melting of ice, indicating that the solution is undersaturated with TBAB such that significant excess water exists after the hydrate component forms as the sample is cooled. When the sample is pressurized with H_2 gas, the hydrate dissociation peak begins to broaden and shift to higher temperature. At 13.79 MPa, there is some evidence of a second hydrate decomposition peak. The area of the ice peaks does not appear to change significantly, suggesting that the partitioning of the sample between hydrate and ice is not affected much by increasing pressure.

No ice peak is detected in the thermograms shown in Figure 15, indicating that at 3.59 mol % TBAB (i.e., TBAB:water ratio of 1:27), there is no excess water. At this concentration, TBAB has been reported to form two types of hydrates: Type A and Type B [7]. The thermograms, however, exhibit three peaks, possibly suggesting three hydrate structures. Since these three peaks can be detected in the atmospheric pressure case where there is no H_2 gas, it is unclear to what extent hydrogen is being incorporated into the hydrate matrix. The general shape of the curves does not change significantly with increasing pressure, although there appears to be a subtle shift in the relative strengths of the second and third peaks, as well as the expected shift to higher melting temperatures.
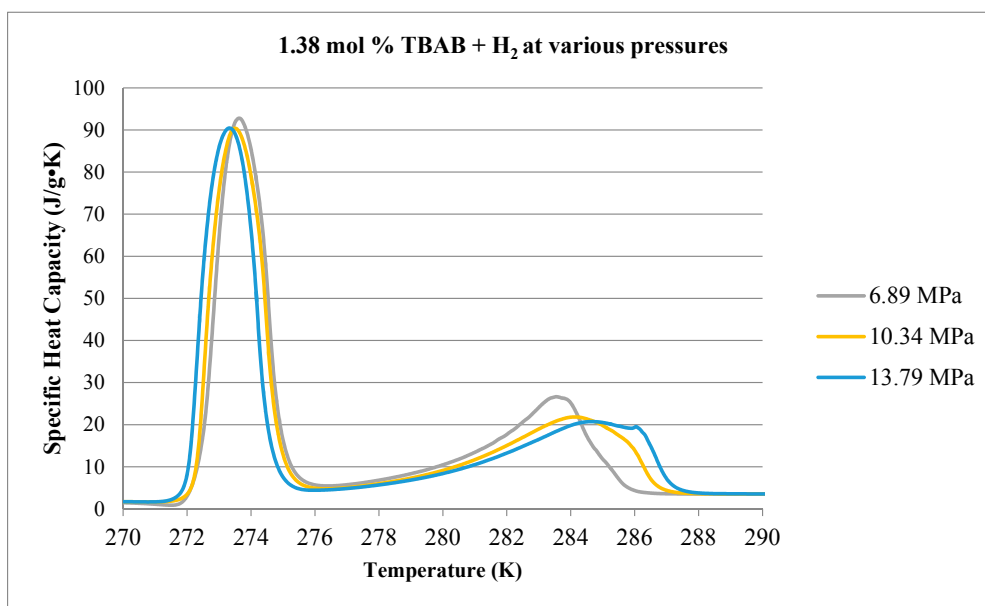
1.38 mol % TBAB + H$_2$ at various pressures

Figure 14. Comparison of decomposition curves for 1.38 mol % TBAB at various hydrogen pressures. Baseline case conducted at atmospheric pressure with no H$_2$.
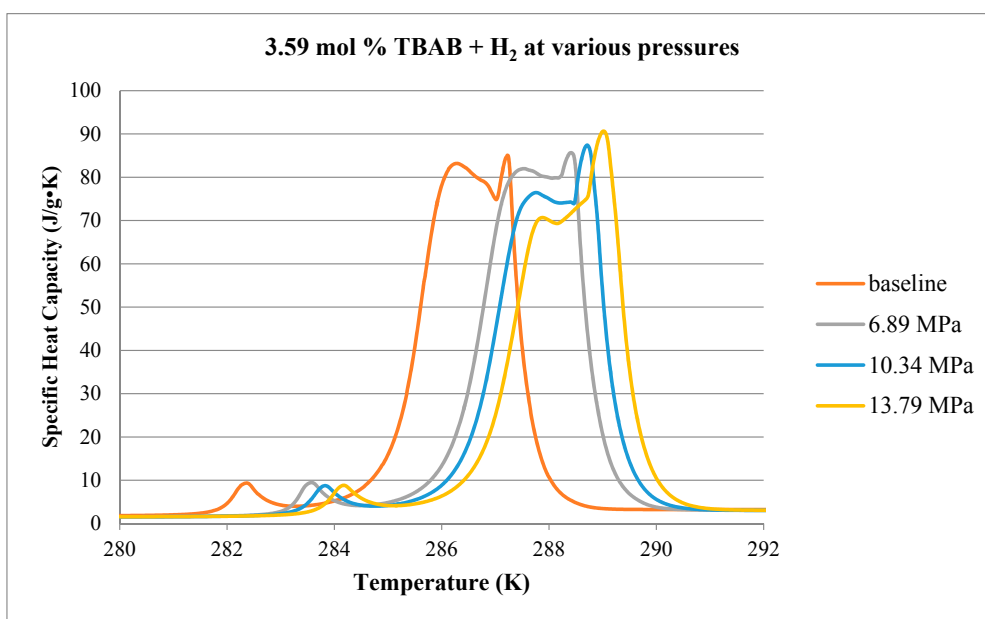
3.59 mol % TBAB + H$_2$ at various pressures

Figure 15. Comparison of decomposition curves for 3.59 mol % TBAB at various hydrogen pressures. Baseline case conducted at atmospheric pressure with no H$_2$.

The calorimetry experiments suggest that pressurization of THF solution with H$_2$ gas during the hydrate formation process results in significant changes in the dissociation thermograms. At the two higher concentrations of THF, a second hydrate peak appears at temperatures between around 280 K and 285 K that increases in strength with increasing pressure. This suggests an additional hydrate structure, possibly due to the incorporation of H$_2$ into the crystal matrix. On the other hand, thermograms of the TBAB solutions did not exhibit conclusive evidence of changes in structure when pressurized with H$_2$. While this does not preclude the possibility of binary TBAB + H$_2$ hydrate formation, it was decided

that THF would be a better candidate for our scale-up tests. One advantage that TBAB has over THF is the slightly higher melting point of the hydrate (about 4 K) at the same pressure.

3.2. Raman Spectroscopy

Calorimetry data indicated that an additional hydrate decomposition peak appears when the 5.56 mol % and 8.34 mol % THF solutions were pressurized with H_2 gas. It was posited that this peak is associated with H_2 in the hydrate phase. Raman spectroscopy experiments were performed to test this hypothesis by confirming the existence of H_2 binary hydrate under conditions where the thermogram peak was detected.

Following procedures described above, Raman spectra were taken at various stages of the gas hydrate dissociation process. Fine ice crystals of 5.56 mol % THF were slowly pressurized with H_2 gas to 6.89 MPa at 263 K and an initial spectrum was collected before significant uptake of hydrogen by the solid phase occurred. This spectrum is shown in Figure 16, which plots light intensity measured by the CCD detector, in arbitrary units (a.u.), as a function of the Raman shift (cm^{-1}). In the gas phase overlying the ice and (pure) THF hydrate, four peaks are detected at 4128, 4146, 4158, and 4165 cm^{-1} which corresponds to the H-H stretching modes of the H_2 molecules. Hydrogen hydrate was then allowed to form. Figure 17 presents a spectrum of the resulting hydrate at 274 K. The broad peak around 4133 cm^{-1} was observed previously by Lee et al. [8] and is due to the entrapment of H_2 in small cages of the binary hydrate. The sample was depressurized and vented and a final spectrum was taken of the 5.56 mol % THF solution at 298 K for comparison. This spectrum is shown in Figure 18. These results appear to confirm the formation of the binary hydrogen hydrate.
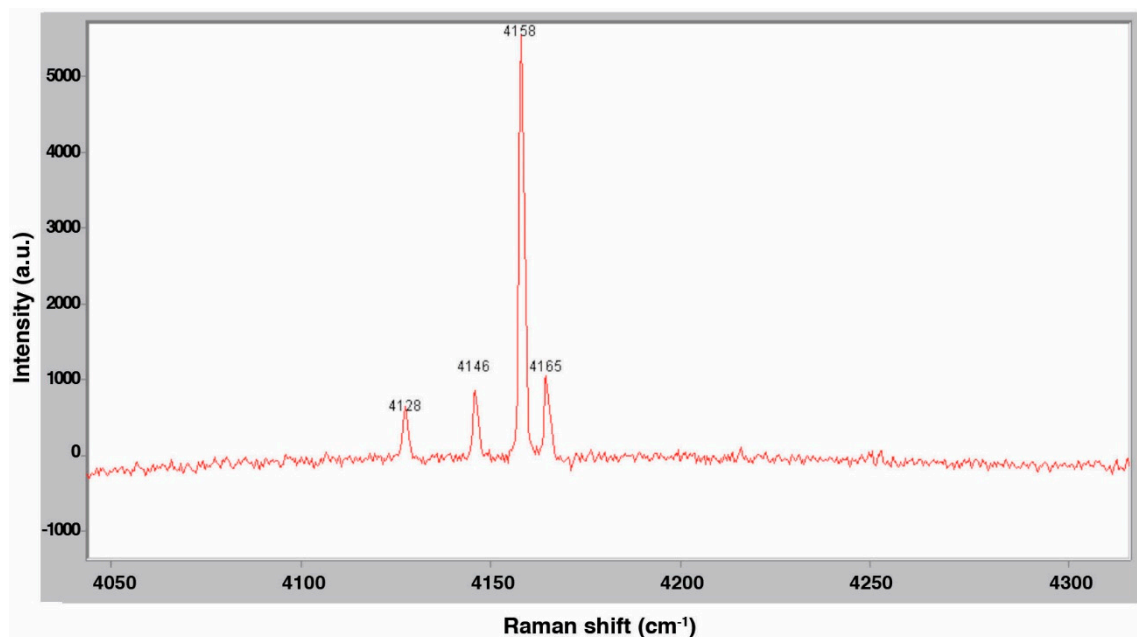

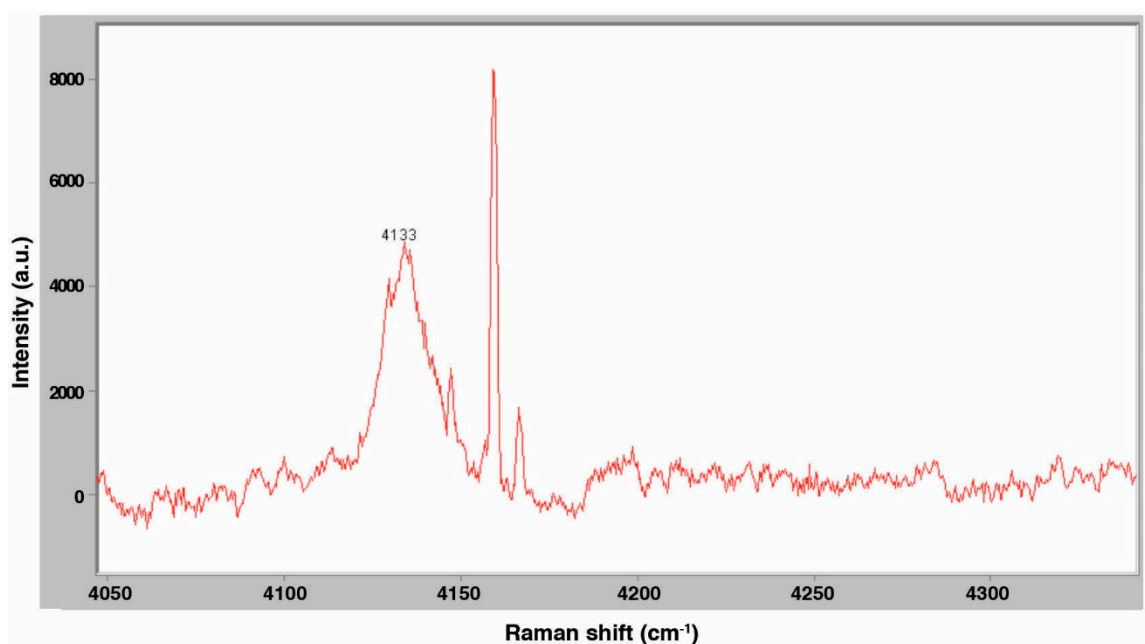**Figure 16.** Raman spectrum of H_2 in the gas phase at 263 K.

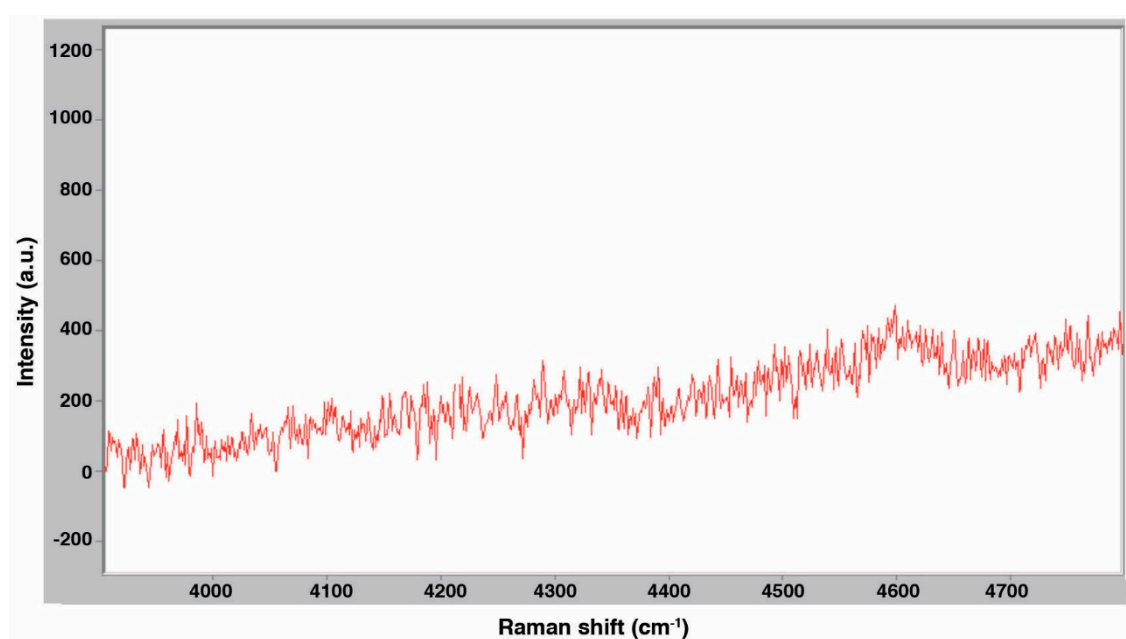**Figure 17.** Raman spectrum of 5.56 mol % THF at 274 K and 6.89 MPa.

Figure 18. Raman spectrum of 5.56 mol % THF solution at 298 K.

3.3. Scale-Up

Scale-up experiments were conducted to estimate the amount of H_2 stored in THF binary hydrates. Quantifying H_2 content is not possible with the MCDSC system. Table 1 summarizes the H_2 storage capacity of 2.78, 5.56, and 8.34 mol % THF hydrate determined from GC analysis of gas samples collected from replicate experiments. In these experiments, the samples were pressurized with pre-cooled H_2 gas to 12 MPa, which falls between the two highest pressures tested with the MCDSC. Due to the pressure ratings of certain components in the scale-up facility flowtrain, a safe operating limit of approximately 2000 psig (13.9 MPa absolute) was established for the system. 12 MPa (gauge) was

selected to accommodate the possibility of pressure excursions within this safety limit. As described previously, gas samples collected at the end of the N_2 purge process at 274 K are analyzed to determine the number of moles of any residual H_2 in the gas phase, based on the measured concentration, pressure, temperature, and known volume of gas in the lines and reactor head space. This is subtracted from the number of moles of H_2 collected after the hydrate fully dissociates (determined from the GC data) to estimate the amount of hydrogen that was stored in the hydrate.

Table 1. Binary hydrogen storage capacity determined from gas sampling and GC analyses.

THF Concentration (mol %)	Sample Size (g)	Δn (mol)	H_2 (g)	Storage Capacity (wt %)
2.78	165	0.041	0.083	0.050
5.56	166	0.022	0.045	0.027
8.34	168	0.022	0.045	0.027

In Table 1, Δn is the number of moles of hydrogen stored in the hydrate sample. The weight % given in the last column on the right is calculated by dividing the total mass of H_2 determined to have been stored in the hydrate by the mass of the fine crystals loaded into the reactor at the start of the experiment. Based on the MCDSC results, a portion of 2.78 mol % and 5.56 mol % samples probably consisted of ice, rather than hydrate. Since this fraction is unknown, however, the total sample mass was used as a basis for comparison of the results.

These results suggest that, while H_2 can be stored in THF binary hydrate, the yield is low. The weight percentages fall far below the 2015 USDOE target of 5.5 weight %. It is interesting to note that the most dilute THF solution (2.78 mol %) had the highest hydrogen storage capacity. The binary gas hydrate formed from this solution released approximately 0.083 g of H_2, corresponding to a 0.05 wt % storage capacity. Increasing the THF concentration to 5.56 mol % THF lowers the gas storage capacity by a factor of two. For 5.56 mol % THF, dissociation of the hydrate released approximately 0.045 g of H_2, corresponding to 0.027 wt % storage capacity. The 8.34 mol % THF supersaturated solution also had a storage capacity of about 0.027 wt %, suggesting that increasing the THF concentration beyond stoichiometric proportions does not necessarily improve H_2 yield.

In consideration of the unexpectedly low H_2 storage capacities determined by gas sampling and analysis, the experimental pressure records were examined to try to estimate H_2 gas uptake during the hydrate formation process to confirm these results. During the formation process, a pressure drop occurs at constant temperature due to the entrapment of H_2 in S-cages generated by (sII) THF hydrate. Since the volume occupied by the isothermal gas in the reactor is fixed, the change in the number of moles of H_2 in the gas results in a decrease in pressure. The Ideal Gas Law was employed to estimate the decrease in moles of H_2 from the measured temperature, pressure drop, and known gas volume, using an appropriate compressibility factor:

$$\Delta n = (\Delta P \times V)/(Z \times R \times T) \tag{1}$$

where Δn is the change in the number of moles of H_2 due to uptake by the hydrate, ΔP is the measured pressure drop, V is the volume of the gas space (98.3 cm^3) that was determined by filling the closed system with fluid and collecting and measuring the volume of that fluid, T is the measured temperature, R is the gas constant, and Z is the calculated compressibility factor, which is approximately 1.09 at the tested hydrate formation conditions.

The formation process for 2.78 mol % THF is shown as an example in Figure 19. Measured H_2 gas pressure data are plotted as a function of temperature. At the start of the experiment, point A, H_2 pressure in the system is 11.15 MPa and sample temperature is about 274 K. As the sample temperature is cooled rapidly from 274 K to 263 K (point B), H_2 gas pressure drops slightly due to the cooling effect. From point B to point C, H_2 is drawn into and trapped in the S-cages of the THF hydrate, resulting in a reduction of gas pressure from slightly more than 11 MPa to slightly less than 10.4 MPa.

Applying the above equation, this corresponds to the uptake of about 0.060 g of H_2. Note that the oscillation in the curve during this period reflects the temperature control characteristics of the freezer. The system temperature is then raised to 277 K. By comparison with Figure 10, this should melt any ice but preserve most of the hydrate. The sample is held at this temperature for 4 h to promote the formation of more hydrate, then cooled to 274 K and held for an additional 24 h. Figure 20 shows a second, smaller pressure drop that is recorded at 274 K. During this process, an additional 0.036 g of H_2 is consumed, for a total of 0.096 g. This value compares reasonably well with GC results of 0.083 g of H_2 released during dissociation.
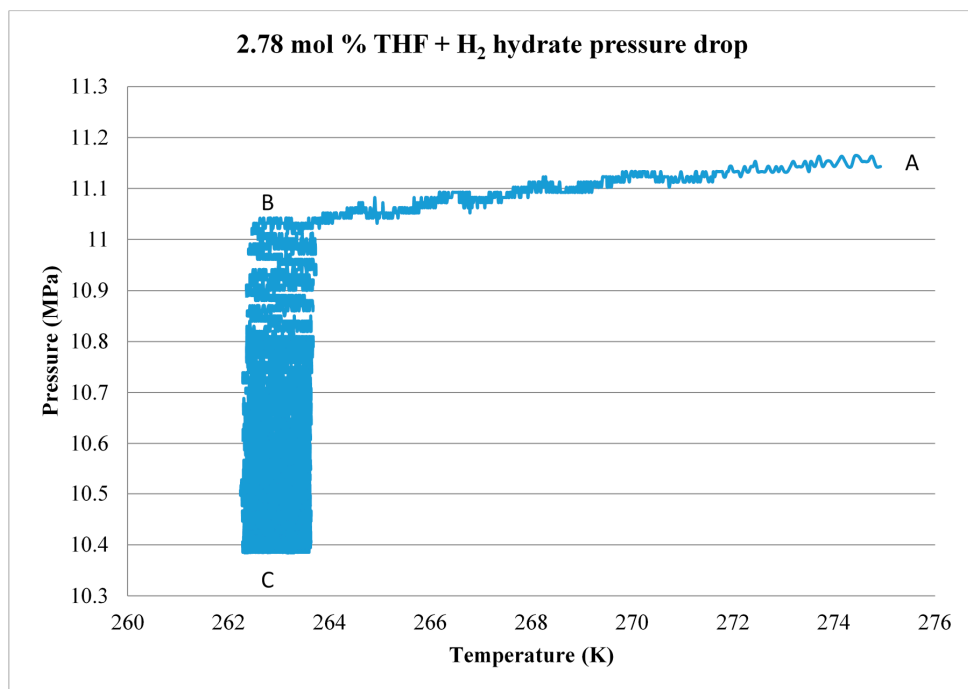

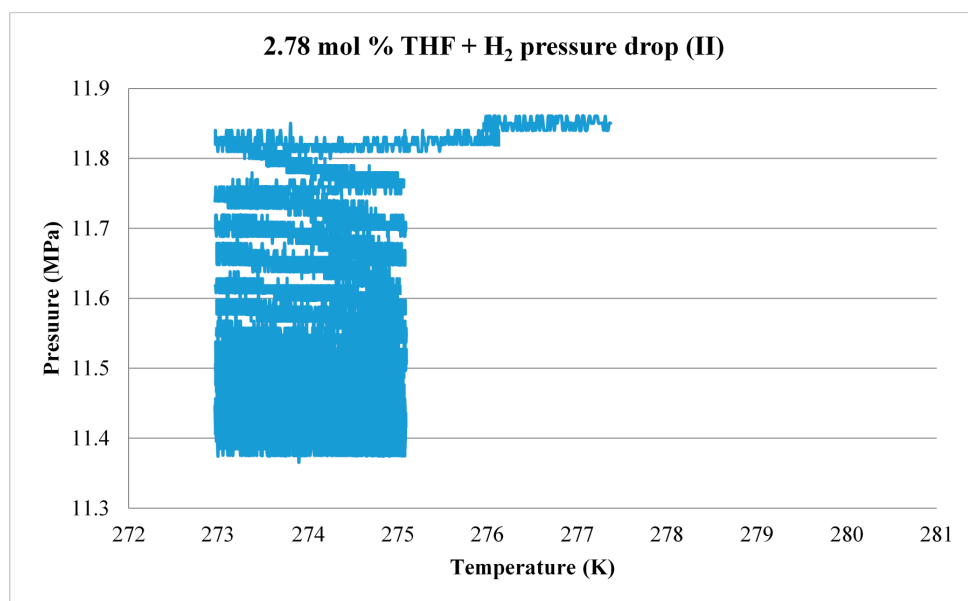**Figure 19.** H_2 gas pressure drop at 263 K due to hydrate formation; 2.78 mol % THF.

Figure 20. H_2 gas pressure drop at 274 K due to hydrate formation; 2.78 mol % THF.

Table 2 compares the results of the gas sampling and pressure drop analyses. While differences are apparent between these two methods, the results compare reasonably well and seem to confirm that, for the specific protocols and conditions examined in this exploratory study, it was not possible to produce binary THF + H_2 hydrate with significant H_2 storage capacity. The measured values in the present scale-up tests are four to ten times smaller than results reported for previous experimental studies conducted at similar THF concentrations, pressures, and temperatures [13,24], and which have been predicted by Grand Canonical Monte Carlo simulations performed recently by Papadimitriou et al. [25]. Although the binary hydrate formation process was allowed to proceed for more than 40 h, kinetic effects may have contributed to the discrepancy. In addition, given the relatively large scale of the reactor, incomplete contact and associated mass transfer restrictions between the H_2 gas phase and sections of the solid ice-hydrate matrix could have limited H_2 uptake.

Table 2. Comparison of binary THF hydrate hydrogen storage capacity at 11 MPa and for three different THF solutions determined by gas sampling and pressure drop analysis.

THF Concentration (mol %)	Sample Size (g)	Gas Sampling Results		Gas Pressure Drop Results	
		H_2 (g)	Storage Capacity (wt %)	H_2 (g)	Storage Capacity (wt %)
2.78	165	0.083	0.050	0.096	0.058
5.56	166	0.045	0.027	0.076	0.046
8.34	168	0.045	0.027	0.064	0.038

4. Conclusions

An exploratory investigation was conducted to evaluate the feasibility of employing binary hydrates as a medium for H_2 storage. Two hydrate promoters, THF and TBAB, which had been reported previously to have potential to form binary hydrates with H_2, were investigated. Aqueous solutions of THF and TBAB at concentrations extending from under-saturated to super-saturated with respect to proportions needed to form hydrate were tested at pressures up to 13.8 MPa. Results from a series of calorimetry experiments suggested that THF forms a binary hydrate with H_2; results for TBAB were not definitive. The measured THF+H_2 hydrate stability data agreed well with the results of Hashimoto et al. [26] and Anderson et al. [27]. To confirm that binary THF + H_2 hydrates had formed in the calorimetry experiments, Raman spectra were taken at different points of the hydrate synthesis process using a separate facility. The spectra exhibited the signature characteristic of H_2 entrapment in the small cages of binary hydrate.

Based on the calorimetry and Raman results, it was decided to focus on solutions of THF and to conduct scale-up experiments to determine H_2 storage capacity. Three solutions of THF (2.78, 5.56, and 8.34 mol %) were tested at pressures up to about 11 MPa over a >40 h hydrate synthesis process. GC and pressure drop analyses confirmed that H_2 was stored in the solid phase. The measured hydrogen storage capacities, unfortunately, were very low. Weight percentages of H_2 in hydrate were less than 0.1%. Interestingly, the unsaturated solution of THF appeared to store the most hydrogen. The reason for this is not clear, although it might be posited that this is related to the lower occupancy of the hydrate cages.

Although the present results are not encouraging from the perspective of employing THF binary hydrate for H_2 transportation applications, it is clear that promoters are successful in significantly shifting the operational pressures and temperature of hydrogen hydrates to values that are feasible for a host of other H_2 storage applications. In consideration of this, additional work appears to be warranted on other binary hydrate storage options for H_2. Possible topics include:

- Add surfactants to the solutions, since recent studies have shown that surfactants can promote the formation kinetics of binary hydrates.
- Conduct extended scale-up experiments that include multiple formation and dissociation cycles and longer hold times to overcome kinetic limitations.

- Conduct scale-up tests with TBAB solutions.

References

1. Schüth, F. Technology: Hydrogen and hydrates. *Nature* **2005**, *434*, 712–713. [CrossRef] [PubMed]
2. Shariati, A.; Raeissi, S.; Peters, C.J. Clathrate Hydrates, Chapter 3. In *Handbook of Hydrogen Storage: New Materials for Future Energy Storage*, 1st ed.; Hirscher, M., Ed.; Wiley VCH: Weinheim, Germany, 2010; pp. 63–79. ISBN 978-3-527-32273-2.
3. Hu, Y.H.; Ruckenstein, E. Clathrate hydrogen hydrate-a promising material for hydrogen storage. *Angew. Chem. Int. Ed.* **2006**, *45*, 2011–2013. [CrossRef] [PubMed]
4. Veluswamy, H.P.; Kumar, R.; Linga, P. Hydrogen storage in clathrate hydrates: Current state of the art and future directions. *Appl. Energy* **2014**, *122*, 112–132. [CrossRef]
5. Florusse, L.J.; Peters, C.J.; Schoonman, J.; Hester, K.C.; Koh, C.A.; Dec, S.F.; Marsh, K.N.; Sloan, E.D. Stable low-pressure hydrogen clusters stored in a binary clathrate. *Science* **2004**, *306*, 469–471. [CrossRef] [PubMed]
6. Hashimoto, S.; Sugahara, T.; Moritoki, M.; Sato, H.; Ohgaki, K. Thermodynamic stability of H_2+tetra-*n*-butyl ammonium bromide mixed gas hydrate in nonstoichiometric aqueous solutions. *Chem. Eng. Sci.* **2008**, *63*, 1092–1097. [CrossRef]
7. Shimada, W.; Shiro, M.; Kondo, H.; Takeya, S.; Oyama, H.; Ebinuma, T.; Narita, H. Tetra-*n*-butylammonium bromide-water. *ACTA Crystollogr. C* **2005**, *61 (Pt 2)*, o65–o66. [CrossRef] [PubMed]
8. Lee, H.; Lee, J.W.; Kim, D.Y.; Park, J.; Seo, Y.T.; Zeng, H.; Moudrakovski, I.L.; Ratcliffe, C.I.; Ripmeester, J.A. Tuning clathrate hydrates for hydrogen storage. *Nature* **2005**, *434*, 743–746. [CrossRef] [PubMed]
9. Strobel, T.A.; Taylor, C.J.; Hester, K.C.; Dec, S.F.; Koh, C.A.; Miller, K.T.; Sloan, E.D. Molecular hydrogen storage in binary THF-H_2 clathrate hydrates. *J. Phys. Chem. B* **2006**, *110*, 17121–17125. [CrossRef] [PubMed]
10. Hester, K.C.; Strobel, T.A.; Sloan, E.D.; Koh, C.A.; Huq, A.; Schultz, A.J. Molecular hydrogen occupancy in binary THF-H_2 clathrate hydrates by high resolution neutron diffraction. *J. Phys. Chem. B* **2006**, *110*, 14024–14027. [CrossRef] [PubMed]
11. Hawkins, R.E.; Davidson, D.W. Dielectric relaxation in the clathrate hydrate of some cyclic ethers. *J. Phys. Chem.* **1966**, *70*, 1889–1894. [CrossRef]
12. Gough, S.R.; Davidson, D.W. Composition of tetrahydrofuran hydrate and the effect of pressure on the decomposition. *Can. J. Chem.* **1971**, *49*, 2691–2699. [CrossRef]
13. Ogata, K.; Hashimoto, S.; Sugahara, T.; Moritoki, M.; Sato, H.; Ohgaki, K. Storage capacity of hydrogen in tetrahydrofuran hydrate. *Chem. Eng. Sci.* **2008**, *63*, 5714–5718. [CrossRef]
14. Dyer, C.K. Fuel cells for portable applications. *Fuel Cells Bull.* **2002**, *2002*, 8–9. [CrossRef]
15. Cheng, X.; Shi, Z.; Glass, N.; Zhang, L.; Zhang, J.; Song, D.; Liu, Z.-S.; Wang, H.; Shen, J. A review of PEM hydrogen fuel cell contamination: Impacts, mechanisms, and mitigation. *J. Power Sources* **2007**, *165*, 739–756. [CrossRef]
16. Schlapbach, L.; Züttel, A. Hydrogen-storage materials for mobile applications. *Nature* **2001**, *414*, 353–358. [CrossRef] [PubMed]
17. Mao, W.L.; Koh, C.A.; Sloan, E.D. Clathrate, hydrates under pressure. *Phys. Today* **2007**, *60*, 42–47. [CrossRef]
18. U.S. Department of Energy, Office of Energy Efficiency and Renewable Energy. Available online: http://www1.eere.energy.gov/hydrogenandfuelcells/storage/pdfs/targets_onboard_hydro_storage_explanation.pdf (accessed on 31 December 2009).
19. Willow, S.Y.; Xanheas, S.S. Enhancement of hydrogen storage capacity in hydrate lattices. *Chem. Phys. Lett.* **2012**, *525–526*, 13–18. [CrossRef]

20. Weissman, J.T. Hydrogen Storage Capacity of Tetrahydrofuran and Tetra-*N*-Butylammonium Bromide Hydrates at Favorable Thermodynamic Conditions. Master's Thesis, University of Hawaii, Honolulu, HI, USA, May 2014.

21. Du, J.; Wang, L.; Liang, W.; Li, D. Phase equilibria and dissociation enthalpies of hydrogen semi-clathrate hydrate with tetrabutyl ammonium nitrate. *J. Chem. Eng. Data* **2011**, *57*, 603–609. [CrossRef]

22. Kim, D.; Park, Y.; Lee, H. Tuning clathrate hydrates: Application to hydrogen storage. *Catal. Today* **2007**, *120*, 257–261. [CrossRef]

23. Sloan, E.D.; Koh, C.A. *Clathrate Hydrates of Natural Gases*, 3rd ed.; CRC Press: Boca Raton, FL, USA, 2008; ISBN 9780849390784.

24. Mulder, F.M.; Wagemaker, M.; van Eijck, L.; Kearley, G.J. Hydrogen in porous tetrahydrofuran clathrate hydrate. *ChemPhysChem* **2008**, *9*, 1331–1337. [CrossRef] [PubMed]

25. Papadimitriou, N.I.; Tsimpanogiannis, I.N.; Economou, I.G.; Stubos, A.K. Storage of H_2 in clathrate hydrates: Evaluation of different force-fields used in Monte Carlo simulations. *Mol. Phys.* **2017**, *115*, 1274–1285. [CrossRef]

26. Hashimoto, S.; Sugahara, T.; Sato, H.; Ohgaki, K. Thermodynamic stability of H_2+Tetrahydrofuran mixed gas hydrate in nonstoichiometric aqueous solutions. *J. Chem. Eng. Data* **2007**, *52*, 517–520. [CrossRef]

27. Anderson, R.; Chapoy, A.; Tohidi, B. Phase relations and binary clathrate hydrate formation in the system $H_2-THF-H_2O$. *Langmuir* **2007**, *23*, 3440–3444. [CrossRef] [PubMed]